Innate immune signaling in trophoblast and decidua organoids defines differential antiviral defenses at the maternal-fetal interface

Liheng Yang[1†], Christina Megli[2,3], Carolyn B. Coyne[1†*]

[1]Department of Pediatrics, University of Pittsburgh School of Medicine, [2]Division of Maternal-Fetal Medicine, Division of Reproductive Infectious Disease, Department of Obstetrics, Gynecology and Reproductive Sciences, University of Pittsburgh Medical Center (UPMC),[3]Magee Womens Research Institute, Pittsburgh, PA USA

[†]Current address: Department of Molecular Genetics and Microbiology, Duke University School of Medicine, Durham, NC USA

*Address correspondence
Carolyn Coyne, PhD
3130 Medical Sciences Research Building III
3 Genome Court
Durham, NC 27710
USA
carolyn.coyne@duke.edu

Abstract

Infections at the maternal-fetal interface can directly harm the developing fetus and compromise the health of the pregnant woman. Innate immune signaling by both fetal-derived placental trophoblasts and the maternal decidua must provide antimicrobial defenses at this critical interface without compromising its integrity. Here, we developed trophoblast and decidua organoids from matched human placentas to define their relative contributions to innate immune defenses at the maternal-fetal interface. We show that trophoblast and decidua organoids recapitulate some, but not all, of the basal cytokine release observed in matched tissue explants. We further show that trophoblast, but not decidua, organoids constitutively release antiviral type III interferons (IFNs) and that fetal and maternal organoids differentially respond to viral infections through the induction of organoid-specific cytokines. These findings define key differences in innate immune signaling generated by fetal-derived trophoblasts and the maternal decidua, which together must protect the fetus from viral infections.

Introduction

The maternal-fetal interface is comprised of both the maternal-derived decidua and the fetal-derived placenta, which together support fetal growth and provide immunologic defenses that protect the fetus from infections. The relative contributions of specific maternal- and fetal-derived cells to these critical functions remain largely undefined given the limitations of models that recapitulate the complex nature of this interface.

The placenta forms a key barrier to viral vertical transmission throughout pregnancy and is comprised in part by fetal-derived trophoblast cells. Trophoblast stem cells located in chorionic villi, the branch like projections that directly contact maternal blood, give rise to cytotrophoblasts (CTBs), the proliferative mononuclear cells of the placenta, extravillous trophoblasts (EVTs), and the syncytiotrophoblast (STB), a multinucleated contiguous cell layer that covers the villous surfaces. EVTs directly remodel the maternal microvasculature to form spiral arteries, which ultimately deliver maternal blood to the surfaces of chorionic villi. Decidualization of the endometrium is required for implantation and appropriate placentation. This process involves the differentiation of fibroblast-like mesenchymal cells into secretory decidua cells. Prior to the formation of chorionic villi and the development of a hemochorial placenta, these secretory cells provide necessary nutrients to the developing embryo (Burton et al., 2002). Together, the decidua and placenta thus provide the fetus with essential hormones and nutrients to support its growth.

While it is clear that the placenta and decidua play complementary roles in fetal development, their contributions to antimicrobial defenses are less well defined. Studies of tissue explants and histopathologic analysis of the placenta suggest that the decidua and chorionic villi have differing roles in the pathogenesis of relevant infections. The decidua may be a primary site of replication for several microorganisms associated with congenital disease, including cytomegalovirus (CMV) (McDonagh et al., 2006; Pereira et al., 2003; Weisblum et al., 2011), Zika virus (ZIKV) (Guzeloglu-Kayisli et al., 2020; Platt et al., 2018; Weisblum et al., 2017), and *Listeria monocytogenes* (Rizzuto et al., 2017), suggesting it may serve as a reservoir for these infections. By contrast, the placenta is

53 largely resistant to infections and possesses a number of intrinsic mechanisms of innate defense. In
54 the case of viruses, human trophoblasts constitutively release antiviral interferons (IFNs) that restrict
55 infection in both autocrine and paracrine manners (Bayer et al., 2016; Corry et al., 2017). These
56 IFNs are of the type III class, which include IFNs-λ1-3 in humans (Lazear et al., 2019; Wells and
57 Coyne, 2018). Constitutive release of IFNs is a unique feature of trophoblasts as IFNs are tightly
58 regulated in most cell types and induced only after detection of the products of viral replication. In
59 mice, type III IFNs also confer protection from Zika virus (ZIKV) vertical transmission and fetal
60 disease, which occurs in a gestational-associated manner (Chen et al., 2017; Jagger et al., 2017),
61 although it is not clear whether mice constitutively release these IFNs. Together, these findings
62 suggest that maternal- and fetal-derived tissue differentially respond to and control viral infections.
63 However, the lack of available models to fully interrogate the differences between maternal- and
64 fetal-derived cells has limited a complete understanding of these processes, including how each
65 tissue type responds to infection.

66 The recent development of trophoblast and decidua organoids from first trimester placental
67 tissue has expanded the models available to study the maternal-fetal interface (Turco et al., 2017;
68 Turco et al., 2018). Previous work has shown that isolation and propagation of trophoblast stem cells
69 from first trimester placental chorionic villi leads to the development of three-dimensional organoids
70 that differentiate to contain all lineages of trophoblast cells present in the human placenta and
71 release well-known pregnancy hormones such as human chorionic gonadotropin (hCG) (Turco et al.,
72 2018). Similarly, decidua organoids isolated from uterine glands recapitulate the transcriptional
73 profile of their tissue of origin and respond to hormonal cues (Turco et al., 2017). These organoid
74 models thus provide ideal systems to profile differences between maternal- and fetal-derived cells,
75 however, these models have not been applied to pathogens infections.

76 To directly compare antiviral signaling pathways between the human placenta and decidua,
77 we generated trophoblast and decidual organoids from matched human placentas and profiled the
78 release of cytokines, chemokines, and other factors from these models under uninfected and virally

infected conditions. In parallel, we performed similar profiling in matched tissue explants from which these organoids were developed and found that organoids recapitulated some, but not all, of the cytokine release profiles of this tissue. To determine whether there are differences in the responses of maternal- and fetal-derived cells to viral infections, we also compared the immunological secretome from organoids treated with a ligand to stimulate toll-like receptor 3 (TLR3) signaling or after infection with ZIKV. These studies revealed that trophoblast organoids selectively secrete the type III IFN IFN-λ2, which does not occur in matched decidua organoids. Moreover, trophoblast and decidua organoids differentially respond to TLR3 activation and ZIKV infection through the secretion of organoid-specific cytokines. Our studies highlight the differential responses of key cells comprising the maternal-fetal interface and provide new models to define the impact of pathogen exposure at this key site.

Results

Establishment and characterization of human trophoblast and decidual organoids

To generate matched human trophoblast organoids (TOs) and decidual organoids (DOs), we used human placental tissue isolated from the second and third trimesters of human pregnancy and cultured stem cells isolated from chorionic villi or isolated decidua in growth factor-containing medium similar to that described previously (Haider et al., 2018; Okae et al., 2018; Sheridan et al., 2020; Turco et al., 2017; Turco et al., 2018) (**Figure 1A**). Isolated stem cells were embedded in Matrigel to allow for self-organization and propagated for ~3 weeks to generate organoid structures that were morphologically similar to those described previously that were isolated from the first trimester (Turco et al., 2017; Turco et al., 2018) (**Figure 1B**). Also similar those isolated from the first trimester (Turco et al., 2018), cultured TOs developed projections that resembled villous structures (**Figure 1B**, arrows at bottom). Confocal microscopy confirmed the three-dimensional architecture of established organoids and verified that TOs expressed markers such as cytokeratin-19 (**Figure 1C**) and DOs expressed markers including cytokeratin-7 and -19 and E-cadherin (**Figure 1D**), consistent with

105 previous reports (Turco et al., 2017; Turco et al., 2018). Also consistent with first trimester tissue-
106 derived TOs (Turco et al., 2018), established mid-to-late gestation TOs differentiated to include
107 various trophoblast lineages, including EVTs, which extended from the TOs to invade the
108 surrounding Matrigel (**Supplemental Figure 1A, 1B**). We confirmed that TOs and DOs expressed
109 markers consistent with their tissue of origin, including the trophoblast specific marker GATA3, which
110 was enriched in TOs but not DOs, and MUC20, which was expressed in DOs but not TOs (**Figure**
111 **1E, 1F**). We also confirmed that TOs, but not DOs, secreted the trophoblast-specific hormone human
112 chorionic gonadotropin (hCG) by both ELISA and rapid test strip assays (**Figure 1G**). Lastly, we also
113 confirmed that TOs secreted pregnancy-specific beta-1 glycoprotein 1 (PSG1), a major product
114 released from the STB, similar to chorionic villous explants (**Figure 1H**) . TOs and DOs could be
115 propagated for at least three months and passaged approximately every 2-3 weeks with stable hCG
116 release (**Supplemental Figure 1C, 1D**). Collectively, these data establish matched TOs and DOs
117 as model systems of the maternal-fetal interface and that they can be isolated from tissue after the
118 first trimester, including from mid-to-late in gestation.
119

120 **Cytokine profiling of TOs and DOs compared to matched tissue explants**

121 We have shown previously that human chorionic villous explants release a number of cytokines,
122 chemokines, and growth factors that impact both maternal and fetal antimicrobial defenses (Megli et
123 al., 2021). Similarly, we have shown that primary human trophoblasts (PHTs) isolated from mid-
124 gestation and full-term placentas secrete some of these same immunoactive factors (Corry et al.,
125 2017; Megli et al., 2021). We therefore profiled the immunological secretome of TOs isolated from
126 three independent placentas and compared these profiles to chorionic villous explants isolated from
127 the same placentas. In addition, we compared these profiles to PHT cells to determine whether there
128 were differences between stem cell-derived trophoblasts and primary trophoblasts isolated directly
129 from full-term tissue. To do this, we used multianalyte Luminex-based profiling for ~80 cytokines,
130 chemokines, growth and other factors from conditioned media (CM) isolated from these models

131 under unstimulated conditions. Factors whose secretion was reliably measured over 50pg/mL were
132 identified as present. We found that TOs secreted two cytokines (IL-6 and IL-28A/IFN-λ2) and three
133 immune-regulated secreted soluble receptors (sTNF-R1, gp130/sIL-6Rβ, sTNF-R2) (**Figure 2A**). By
134 contrast, matched chorionic villous explants were immunologically more active and we reliably
135 detected 51 factors (**Figure 2B**). Similarly, PHT cells also released a greater number of factors, with
136 31 detected (**Figure 2C**). The five factors released from TOs were also released from chorionic
137 villous explants and PHT cells (**Figure 2D**). The most abundant cytokine present in CM isolated from
138 TOs was IL-6, which was released at levels similar to those observed in both chorionic villi and PHT
139 cells (**Figure 2E**). In contrast, whereas the most abundant factor in CM isolated from PHT cells was
140 IL-8, which was also highly abundant in CM from chorionic villi, this cytokine was not detected in CM
141 isolated from TOs, suggesting that there might be differential immune regulation between terminally
142 differentiated PHT cells and those that are stem-cell derived (**Figure 2F**).

143 To define the immunological secretome of DOs, we performed similar Luminex-based
144 profiling as the studies described above from CM isolated from DOs and decidua explants.
145 Compared to TOs, DOs released a larger number of factors overall, with 21 detected in DO-derived
146 CM (**Figure 3A**). Of these, 19 were also released from human decidua explants, which contained
147 50 total cytokines and other factors (**Figure 3B, 3C**). DOs and decidua explant tissue secreted similar
148 levels of factors such as MMP-1 (**Figure 3D**). In contrast, we found that DOs secreted high levels of
149 IL-10, which was not detected in CM from decidua explants (**Figure 3E**). Together, these data
150 suggest that TOs and DOs partially recapitulate the secretion profile of chorionic villi and the decidua.
151

152 **Trophoblast organoids constitutively secrete antiviral IFN-λ2**

153 We next directly compared the secretion profiles from CM collected from matched TOs and DOs to
154 identify factors enriched in either maternal- or fetal-derived cells. TOs selectively secreted two
155 cytokines that were not present in CM isolated from matched DOs, IL-6 and IFN-λ2 (**Figure 4A-B,**
156 **D).** In contrast, DOs selectively released high levels of other factors such as IL-8 (**Figure 4C**). We

157 showed previously that PHT cells isolated from full-term placentas and mid-gestation chorionic villi
158 constitutively release type III IFNs, which protect from viral infections (Bayer et al., 2016; Corry et al.,
159 2017). We found that TOs recapitulated this phenotype and released high levels of IFN-λ2, but not
160 type I IFNs or IFN-λ1 (**Figure 4E**). In contrast, DOs did not basally secrete any detectable IFNs
161 (**Figure 2A, 4D**). We monitored the release of IFN-λ2 over the growth period of TOs and found that
162 it's release was detectable by ~10-days post-plating and reached high levels by >14-days in culture,
163 which correlated with similar trends for IL-6 (**Figure 4F**). We confirmed that CM isolated from TOs,
164 but not DOs, induced interferon stimulated genes (ISGs) using a HEK293 based reporter assay
165 (**Figure 4G**). Consistent with this, we found that CM isolated from TOs was antiviral and reduced
166 ZIKV infections in non-placental cells treated with this CM (**Figure 4H**). PHT cells and villous explants
167 basally express high levels of ISGs, most likely from the autocrine effects of released IFN-λs (Corry
168 et al., 2017). Therefore, we compared the basal expression of two ISGs, IFI44L and OASL, in TOs
169 and DOs and found that TOs expressed significantly higher levels of these ISGs that do DOs (**Figure**
170 **4I**). These data show that TOs recapitulate the constitutive release of type III IFNs observed in
171 primary trophoblast cells and tissue and that these IFNs function in paracrine to restrict viral
172 infections.
173
174 **Differential induction of antiviral signaling in TOs and DOs**
175 Because we observed differences in the constitutive release of IFN-λ2 from TOs and DOs, we next
176 determined how these organoids responded to viral infections. To do this, we used poly (I:C), a
177 synthetic ligand of TLR3 and measured differences in cytokine induction using Luminex-based
178 profiling. We found that both TOs and DOs robustly responded to poly I:C treatment, which
179 corresponded with the induction of ISGs in both models, although TOs induced higher transcript
180 levels of these ISGs (**Supplemental Figure 2A**). Cytokine profiling of CM isolated from poly I:C-
181 treated TOs and DOs showed that TOs induced 15 factors (>5-fold change from mock) and DOs

182 induced 14 factors (>5-fold change from mock) in response to TLR3 activation (**Figure 5A**). Of the
183 factors induced, 9 were shared between both TOs and DOs (**Figure 5B**), which included IFN-λ1,
184 which was the most induced cytokine in both organoids (**Figure 5C**) and IFN-λ2 (**Figure 5D**). Several
185 cytokines were differentially induced in TOs versus DOs, including IFN-γ, which was induced in DOs
186 but not TOs (**Supplemental Figure 2B)** and IL-8**,** which was induced in TOs but not DOs
187 (**Supplemental Figure 2C).** In addition, we found that whereas TOs induced the type I IFNs IFN-α2
188 and IFN-β in response to poly I:C, DOs induced no IFN-α2 and low levels of IFN-β (**Figure 5E, 5F,**
189 **Supplemental Figure 2A**).

190 We next profiled the differential response to viral infections in TOs and DOs using ZIKV. We
191 found that both TOs and DOs supported ZIKV replication as assessed by the presence of viral RNA
192 by qPCR at 72hrs post-infection (p.i.) (**Figure 6A**). Luminex-based profiling of CM isolated from these
193 cultures at 24hrs, 48hrs, and 72hrs p.i. showed that few cytokines were induced by ZIKV infection
194 and no cytokines or other factors were induced >5-fold (**Figure 6B, 6C**). Consistent with poly I:C
195 treatment, TOs induced very low levels of IFN-λ1 and IFN-β at 72hrs p.i., which was not observed in
196 DOs (**Figure 6D**). Consistent with this, we observed low level induction of ISGs in TOs that was not
197 observed in DOs (**Supplemental Figure 2D**). In contrast, DOs secreted low levels of the
198 glycophosphoprotein osteopontin at 24hrs p.i., which decreased over the course of infection (**Figure**
199 **6F**). Taken together, these data show that TOs and DOs differentially respond to viral infections
200 through the release of select cytokines and other factors.

201

202 **Differential response to IFNs in TOs and DOs**

203 Previous work has shown that chorionic villous and decidua explants respond to treatment with
204 recombinant IFNs, which protect from ZIKV infection (Jagger et al., 2017), although villous explants
205 appear to be less responsive to type III compared to type I IFNs (Yockey et al., 2018). However,
206 given that the tissue used in these studies contains many different cell types, we investigated the

207 sensitivity of TOs and DOs to recombinant type I (IFN-β) or type III (IFN-λ) treatment. We found that
208 DOs were highly responsive to both type I and III IFN treatment and robustly induced ISGs including
209 IFI44L and OASL (**Figure 7A, 7B**). These ISGs were similarly induced by IFN treatment of decidua
210 explants (**Figure 7C**). Although TOs did respond to both type I and III IFN treatment, the magnitude
211 of these responses were lower than those in DOs (**Figure 7A, 7B**), which were consistent with the
212 responses of IFN-treated chorionic villous explants (**Figure 7C, 7D**). These data suggest that there
213 are differences in the sensitivity of maternal-and fetal-derived cells to type I and III IFNs.
214

215 **Discussion**

216 Our work presented here establishes fetal- and maternal-derived organoids as models of innate
217 immune signaling at the maternal-fetal interface. We show that TOs constitutively secrete only two
218 cytokines, including the pro-inflammatory cytokine IL-6 and antiviral IFN-λ2. In contrast, we show
219 that DOs are immunologically more active under resting conditions and basally secrete a number of
220 cytokines not observed in TOs, but do not release IFNs under unstimulated conditions. In addition,
221 we show that TOs and DOs differentially respond to TLR3 activation and ZIKV infection and induce
222 organoid-specific cytokines in response to activation of antiviral innate immune signaling. Collectively,
223 our work suggests that cells that comprise the maternal-fetal interface defend from viral infections in
224 a cell-type specific manner and highlight the unique contributions of fetal-derived trophoblasts in
225 antiviral immunity.

226 The previous establishment of trophoblast and decidua-derived organoids has significantly
227 expanded the *in vitro* systems that can model the complexity of the maternal-fetal interface (Turco
228 et al., 2017; Turco et al., 2018). These previous studies utilized tissue isolated from the first trimester
229 of pregnancy (6-9 weeks gestation for TOs and 8-12 weeks gestation for DOs) (Turco et al., 2017;
230 Turco et al., 2018). Here, we show that these organoids can also be isolated from later stages of
231 gestation, including from full-term placental tissue. Moreover, we show that the growth medium and

232 conditions used to grow organoids from first trimester tissue can be extrapolated to grow organoids
233 from the second and third trimesters of pregnancy. Two-dimensional cultures of stem cell-derived
234 primary trophoblasts are also restricted to tissue obtained in the first trimester (Okae et al., 2018).
235 Given that access to first trimester tissue can be complicated by access an/or regulatory restrictions,
236 our studies provide an additional source for the development of placental organoids from tissue
237 obtained later in gestation. Moreover, the establishment of these organoids from tissues later in
238 gestation may allow for elucidation of the role of maternal-fetal signaling in obstetric related
239 pathologies.

240 Unlike many other barrier cell types such as the epithelium, human trophoblasts have the
241 unique capacity to robustly secrete cytokines and other immunological factors without stimulation.
242 Primary human trophoblasts from full-term placentas and mid-gestation chorionic villi secrete a
243 number of cytokines that mediate innate defenses from bacteria, parasites, and viruses (Ander et al.,
244 2018; Bayer et al., 2016; Megli et al., 2021). Consistent with this, serum isolated from pregnant
245 women often contains elevated levels of these cytokines, indicating that at least some have reached
246 the systemic circulation (Benyo et al., 2001; Liu et al., 2019; Megli et al., 2021; Vassiliadis et al.,
247 1998). Similarly, the decidua releases specific cytokines and alterations in these profiles may be
248 associated with pregnancy complications including miscarriage (Alam et al., 2008; Denison et al.,
249 1998; Laham et al., 1997; Lash and Ernerudh, 2015; Pitman et al., 2013; von Rango et al., 2003).
250 The decidua also responds to microbial infections via the release of additional cytokines that function
251 in innate defense (Barber et al., 2005; Guzeloglu-Kayisli et al., 2020; Qiu et al., 2009). However, in
252 many cases, these studies were performed on tissue explants that were multicellular in nature, thus
253 preventing an assessment of the contributions of cytokine release from distinct cell types. Similarly,
254 previous work utilizing tissue explants that are treated with recombinant cytokines, synthetic ligands
255 of various innate immune pathways, or infected with pathogens are also unable to define the
256 contributions of distinct cell types in these responses. The use of organoids therefore allows for
257 analyses of cellular responses to infection or innate immune activation from trophoblasts and

258 decidual glands in primary cell models that contain isolated cell types enriched at the maternal-fetal
259 interface. An additional strength of the TO model is that trophoblast stem cells differentiate into all
260 three distinct trophoblast cell types comprising the human placenta (Turco et al., 2018), which is not
261 possible in many other existing models including isolation of CTBs from full-term placentas.

262 The constitutive release of IFN-λs from human trophoblasts is a highly unique phenomenon
263 that runs counter to much of what is understood about antiviral IFN signaling, which is centered on
264 a requirement for viral sensing to induce this pathway. Our findings from TOs support that IFN
265 release occurs soon after trophoblast differentiation and is likely an early mechanism used by the
266 placenta to defend from viral infections. However, our studies indicated that TOs and DOs may be
267 similarly permissive to ZIKV infection based on levels of vRNA. Previous work has shown that human
268 CTBs and EVTs are permissive to ZIKV whereas the STB is resistant (Platt et al., 2018; Tabata et
269 al., 2016). Given that TOs contain EVTs, CTBs, and that the STB faces inward in the organoid
270 structure, it is possible that these cells support ZIKV infections in TOs. It remains unknown whether
271 EVTs and CTBs exhibit differential responses to type III IFNs which might impact this differential
272 susceptibility to ZIKV infection. Interestingly, our data also show that TOs constitutively release IFN-
273 λ2 and that IFN-λ1 is only induced upon activation of antiviral signaling pathways. IFN-λs genes are
274 located in tandem on chromosome 19 in humans and the mechanisms that might control the
275 constitutive release of IFN-λ2 specifically in trophoblasts is unclear. Our studies also show that type
276 III IFNs are further induced by activation of antiviral innate immune signaling in both TOs and DOs,
277 with IFN-λ1 being the most induced cytokine detected in both organoid types. However, the type I
278 IFN IFN-β is induced to greater levels in TOs than DOs, suggesting that at least some of the cells
279 that comprise the maternal-fetal interface differentially rely on type I and III IFNs for antiviral defenses.

280 Previous work suggests that type I IFNs damage placental structure and function in mice and
281 induce alterations in placental structure in *ex vivo* human chorionic villi (Yockey et al., 2018). In
282 contrast, type III IFN signaling in mice is protective against viral infections and there are no

283 deleterious effects of treatment of pregnant animals with recombinant IFN-λs (Chen et al., 2017;
284 Jagger et al., 2017). While the mechanisms for the opposing effects of type I and III IFNs have yet
285 to be fully elucidated, at least one ISG, interferon-induced transmembrane (IFITM), inhibits fusion of
286 CTBs into the STB (Buchrieser et al., 2019; Zani et al., 2019), which may indicate that expression of
287 select ISGs is tightly regulated to prevent IFN-mediated placental damage. Our data in TOs and
288 DOs suggests that trophoblasts and decidual cells exhibit differential responsiveness to recombinant
289 IFN treatment, with treatment of TOs inducing lower levels of ISGs than those observed in DOs.
290 While this might be attributed to reduced expression of the receptors associated with these IFNs in
291 TOs, there might also be additional mechanisms employed by trophoblasts to protect from IFN- and
292 ISG-mediated damage.

293 Our work presented here develops TOs and DOs from mid-to-late gestation placental tissue
294 and demonstrates that these organoids recapitulate some of the immunologic secretory phenotypes
295 of placental tissue isolated from matched placental tissue. We further show that TOs and DOs
296 constitutively secrete unique cytokines and respond to viral infections through the release of
297 organoid-specific cytokines. Our work also highlights the prominent role of type III IFNs in antiviral
298 immunity at the maternal-fetal interface and demonstrates that TOs constitutively release IFN-λ2.
299 Collectively, these studies define the differential responses of key cells comprising the maternal-fetal
300 interface and suggest that organoid-based models can be used to define innate immune signaling
301 at this interface.

302

303 **Materials and Methods**

304 **Human samples**. All human tissue used in this study was obtained through the UPMC Magee-
305 Womens Hospital Obstetric Maternal & Infant Database and Biobank after approval was received
306 from the University of Pittsburgh Institutional Review Board (IRB) and in accordance with the
307 guidelines of University of Pittsburgh human tissue procurement. Placental tissue used in this study

308 was collected from the second (23rd and 27th) and third (38th) trimesters, including from dizygotic
309 twins. Placental tissue was excluded for diagnosis of PPROM, labor, or maternal infection
310
311 **Derivation and culture of trophoblast organoid (TOs) cultures from human placental samples**.
312 Villous trophoblast stem cells were isolated from fresh placental tissues as described previously
313 (Turco et al., 2018). Briefly, villi collected from fresh placental tissue were intensively washed, then
314 were sequentially digested with 0.2% trypsin-250/0.02% EDTA and 1.0 mg/mL collagenase V.
315 Pooled digests were washed with Advanced DMEM/F12 medium (Gibco 12634-010) and pelleted
316 by centrifugation, then resuspended in approximate 10 times volume of ice-cold growth-factor-
317 reduced Matrigel (Corning 356231). Matrigel "domes" (40 µl/well) were plated into 24-well tissue
318 culture plates (Corning 3526), placed in a 37°C incubator to pre-polymerize for ~2 min, turned upside
319 down to ensure equal distribution of the isolated cells in domes for another 10 min, then carefully
320 overlaid with 500 µL prewarmed trophoblast organoid medium (TOM) consisting of Advanced
321 DMEM/F12 (Life Technologies) supplemented with 1× B27 (Life Technologies), 1× N2 (), 2 mM
322 GlutaMAX™ supplement (), 100 µg/mL Primocin, 1.25 mM N-Acetyl-L-cysteine (Sigma), 500 nM
323 A83-01 (Tocris), 1.5 µM CHIR99021 (Tocris), 50 ng/mL recombinant human EGF (Gibco), 80 ng/mL
324 recombinant human R-spondin 1 (R & D systems), 100 ng/mL recombinant human FGF2
325 (Peprotech), 50 ng/mL recombinant human HGF (Peprotech), 10mM nicotinamide (Sigma), 2 µM Y-
326 27632 (Sigma), and 2.5 µM prostaglandin E2 (PGE2, Sigma). Cultures were maintained in a 37°C
327 humidified incubator with 5% CO_2. Medium was renewed every 2-3 days. Small trophoblast organoid
328 spheroids became visible by approximately day 12 post-isolation. Derived TOs were passaged every
329 10 to 14 days depending on their size and density. To passage, TOs were released from domes with
330 ice-cold cell recovery solution (Corning) and then were digested in prewarmed TrypLE Express
331 (Gibco) or Stem Pro Accutase (Gibco) at 37°C for 5-7 min. Further mechanical dissociation was
332 achieved with an Eppendorf Explorer Plus electronic pipettes at its "mix" function setting by pipetting
333 up and down around 400 times through small-bore pipette tips. Dissociated TOs fragment were

334 collected and washed by centrifuge, then resuspended in fresh ice-cold Matrigel and replated as
335 domes at the desired density for continuous culture. For freezing TOs, overlaid TOM was aspirated,
336 TOs with Matrigel were resuspended in CryoStor CS10 stem cell freezing medium (STEMCell
337 Technologies) frozen at -80 ℃ and then transferred to liquid nitrogen for long-term storage. For
338 thawing cryopreserved TOs, TOs were thawed as quickly as possible, diluted with 5 times volume of
339 basic TOM containing Advanced DMEM/F12, 2 mM GlutaMAX supplement, 10 mM HEPES, 1 ×
340 Penicillin/Streptomycin and centrifuged to pellet. Afterwards, TOs were resuspended in new ice-cold
341 Matrigel and replated for recovery culture.
342
343 **Derivation and culture of decidual organoids (DOs) cultures from human decidua samples**.
344 Decidual gland-enriched cell suspension were acquired from fresh decidual tissue as described
345 previously (Turco, 2017; Turco et al., 2017). Briefly, isolated decidual tissues were cut into small
346 pieces then digested in 1.25 U/mL Dispase II (Sigma, D4693)/0.4 mg/mL collagenase V (Sigma, C-
347 9263) solution. Glandular cells were filtered out from the digestion solution supernatant and
348 resuspended in ice-cold Matrigel (Corning, 356231), plated as domes in 24-well plates (Corning
349 3526), and finally overlaid with 500 μL prewarmed organoid Expansion Medium (ExM) with the same
350 composition as previously described(Turco et al., 2017). The growth medium was renewed every 2-
351 3 days. Mature organoids were passaged by mechanically disruption following TrypLE Express
352 (Gibco, 12605) digestion every 7-10 days. Other maintenance were similar to those as previously
353 described (Turco, 2017).
354
355 **Generation of TO and DO conditioned media (CM).** Overlaid TOM and ExM were collected every
356 2-4 days based on the growth status of TOs and DOs. Media from at least ten timepoints for each
357 established organoid lines were collected as TO-CM or DO-CM. Non-conditioned medium (NCM)
358 was TOM or ExM (described above) that had not been exposed to TOs or DOs, respectively.
359

360 **Cells and Viruses.** PHT cells were established and cultured as described previously (Bayer et al.,
361 2016) . Human osteosarcoma U2OS (ATCC HTB-96) and Vero (ATCC CCL-81) cells were grown in
362 Dulbecco's minimal essential medium (DMEM) with 10% FBS and 1% antibiotic. HEK-Blue IFN-λ
363 reporter cells (hkb-ifnl) were purchased from InvivoGen. ZIKV (Paraiba/2015, provided by David
364 Watkins, University of Miami) was propagated in Vero cells. Viral titers were determined by
365 fluorescent focus assay as previously described (Payne et al., 2006) using recombinant anti-double-
366 stranded RNA monoclonal antibody J2 (provided by Abraham Brass, University of Massachusetts).
367 Infection was determined by qRT-PCR as described below. To assess antiviral activity, U2OS cells
368 were exposed to TO or DO CM, or matched NCM, 24 hr prior to infection with ZIKV Paraiba/2015 for
369 72hrs. ZIKV infection of TOs and DOs was performed using 10^6 FFU virus per well for 24-72hrs, as
370 indicated.
371
372 **Immunofluorescence microscopy.** TOs and DOs were released from Matrigel domes with 1 mL of
373 cell recovery solution (Corning, 354253) per well without disrupting their 3D architecture, then were
374 fixed in 4%PFA for 30 min at room temperature, followed by 0.5% Triton X-100/PBS to permeabilize
375 for 30 min at 4°C. Organoids were washed and blocked in 5%(v/v) goat serum/0.1%(v/v) Tween-20
376 in PBS for 15 min at room temperature and then incubated with primary antibodies in the above-
377 described blocking solution at 4°C overnight. Organoids were then washed with PBS and then
378 incubated for 1-2 h at room temperature with Alexa Fluor-conjugated secondary antibodies
379 (Invitrogen). Organoids were washed again with PBS and mounted in Vectashield (Vector
380 Laboratories) containing 4′,6-diamidino- 2-phenylindole (DAPI) and were transferred onto
381 microscope slides with large-orifice 200 µL-tips (Fisher Scientific, 02707134). The following
382 antibodies or reagents were used: cytokeratin-7 (Abcam, ab9021), cytokeratin-19 (Abcam, ab9221),
383 E-cadherin (Invitrogen, PA5-85088), Abcam), Alexa Fluor 594–conjugated phalloidin (Invitrogen,
384 A12381), Alexa Fluor Plus 488 Goat anti-Mouse IgG secondary antibody (Invitrogen, A32723), Alexa
385 Fluor 488 Goat anti-Rabbit IgG secondary antibody (Invitrogen, A11034). Images were captured

386 using a Zeiss LSM 710 inverted laser scanning confocal microscope and contrast-adjusted in
387 Photoshop or Fiji.
388
389 **RNA extraction, cDNA synthesis and quantitative PCR.** Total RNA was extracted with the Sigma
390 GenElute total mammalian RNA miniprep kit following the manufacturer's instruction and using the
391 supplementary Sigma DNase digestion. RNA quality and concentration were determined using a
392 Nanodrop ND-1000 Spectrophotometer. Total RNA was reverse-transcribed with the iScript cDNA
393 synthesis kit (Bio-Rad) following the manufacturer's instructions. Quantitative PCR was performed
394 using the iQ SYBR Green Supermix (Bio-Rad, 1708882) on a CFX96 Touch Real-Time PCR
395 Detection System (Bio-Rad). Gene expression was determined based on a ΔC_T method normalized
396 to actin. Primer sequences for actin, IFN-β, IL-28A/IFN-λ2, IFI44L, OASL, GATA3, MUC20, and ZKIV
397 vRNA have been previously described (Good et al., 2019; Megli et al., 2021). All primer sequences
398 used in this study can be found in Table S1.
399
400 **hCG and PSG1 ELISAs and Luminex assays**. Human hCG (Sigma, RAB0092) and PSG1 (R&D
401 Systems, DY6799) ELISAs were performed according to the manufacturer's instructions. Plates
402 were read at 450 and 520 mm using a Synergy H1 microplate reader. All sample processing was
403 performed in duplicate and each experiment was performed with at least three biological replicates.
404 Luminex assays were performed using the following kits according to the manufacturer's instructions:
405 Bio-Plex Pro Human Inflammation Panel 1, 37-Plex kit (171AL001M; Bio-Rad Laboratories) and Bio-
406 Plex Pro Human Cytokine Screening Panel, 48-Plex kit (12007283; Bio-Rad Laboratories). The
407 plates were read on a MAGPIX (EMD Millipore) Luminex machine and analyzed using xPONENT
408 software (EMD Millipore).
409
410 **IFN-λ activity reporter assay.** For IFN-λ activity detection from CM, HEK-Blue IFN-λ reporter cells
411 were used according to the manufacture's protocol. Briefly, IFN-λ reporter cells were plated into a

412 96-well plate, then CM was added and incubated at 37 °C for 24 hr. Supernatants (20 µl) were
413 collected and then transferred into a 96-well plate and activity measured using QUANTI-Blue
414 Solution (InvivoGen, rep-qbs) after incubating at 37 °C for 2 hr using a spectrophotometer at 655 nm.
415 Each CM preparation was run in triplicate.
416
417 **Recombinant human IFN and poly(I:C) treatment.** For Poly (I:C) treatment, TOs or DOs were
418 incubated with 10 µg/mL Poly (I:C) diluted in organoid complete growth media for ~24 h, then
419 supernatant was collected for Luminex-based multianalyte profiling or RNA isolated as described for
420 qRT-PCR. For recombinant human IFN treatment, TOs or DOs were treated with IFN-β (8499-IF-
421 010; R&D Systems) or IFN-λ3 (5259-IL-025, R&D Systems) for 24 hr, then total RNA was extracted
422 as described above for following qRT-PCR analysis.
423
424 **Statistics and reproducibility.** All experiments reported in this study have been reproduced using
425 independent samples (tissues and organoids) from multiple donors. All statistical analyses were
426 performed using Prism software (GraphPad Software). Data are presented as mean ± SD, unless
427 otherwise stated. Statistical significance was determined as described in the figure legends.
428 Parametric tests were applied when data were distributed normally on the basis of D'Agostino-
429 Pearson analyses; otherwise, nonparametric tests were applied. P values <0.05 were considered
430 statistically significant, with specific P values noted in the figure legends.
431
432 **Author contributions** LY designed and performed experiments and participated in manuscript
433 review and writing, CM performed tissue dissections and participated in manuscript review and
434 writing, and CC designed and performed experiments, participated in manuscript review and writing,
435 and secured funding.
436
437 **Acknowledgements**

We thank Jon Boyle (University of Pittsburgh) for careful review of the manuscript and the Magee Obstetric Maternal & Infant (MOMI) Database and Biobank at the Magee Women's Research Institute (MWRI) for providing placental tissue. This project was supported by NIH AI145828 (C.B.C.) and the Children's Hospital of Pittsburgh of the UPMC Health System (C.B.C). This project also used the UPMC Hillman Cancer Center and Tissue and Research Pathology/Pitt Biospecimen Core and Animal Facility shared resources which are supported in part by award P30CA047904.

464 **Literature Cited**

465

466 Alam, S.M., Konno, T., Sahgal, N., Lu, L., and Soares, M.J. (2008). Decidual cells produce a heparin-
467 binding prolactin family cytokine with putative intrauterine regulatory actions. J Biol Chem *283*,
468 18957-18968.

469 Ander, S.E., Rudzki, E.N., Arora, N., Sadovsky, Y., Coyne, C.B., and Boyle, J.P. (2018). Human
470 Placental Syncytiotrophoblasts Restrict Toxoplasma gondii Attachment and Replication and
471 Respond to Infection by Producing Immunomodulatory Chemokines. mBio *9*.

472 Barber, E.M., Fazzari, M., and Pollard, J.W. (2005). Th1 cytokines are essential for placental
473 immunity to Listeria monocytogenes. Infect Immun *73*, 6322-6331.

474 Bayer, A., Lennemann, N.J., Ouyang, Y., Bramley, J.C., Morosky, S., Marques, E.T., Jr., Cherry, S.,
475 Sadovsky, Y., and Coyne, C.B. (2016). Type III Interferons Produced by Human Placental
476 Trophoblasts Confer Protection against Zika Virus Infection. Cell Host Microbe *19*, 705-712.

477 Benyo, D.F., Smarason, A., Redman, C.W., Sims, C., and Conrad, K.P. (2001). Expression of
478 inflammatory cytokines in placentas from women with preeclampsia. J Clin Endocrinol Metab *86*,
479 2505-2512.

480 Buchrieser, J., Degrelle, S.A., Couderc, T., Nevers, Q., Disson, O., Manet, C., Donahue, D.A., Porrot,
481 F., Hillion, K.H., Perthame, E.*, et al.* (2019). IFITM proteins inhibit placental syncytiotrophoblast
482 formation and promote fetal demise. Science *365*, 176-180.

483 Burton, G.J., Watson, A.L., Hempstock, J., Skepper, J.N., and Jauniaux, E. (2002). Uterine glands
484 provide histiotrophic nutrition for the human fetus during the first trimester of pregnancy. J Clin
485 Endocrinol Metab *87*, 2954-2959.

486 Chen, J., Liang, Y., Yi, P., Xu, L., Hawkins, H.K., Rossi, S.L., Soong, L., Cai, J., Menon, R., and Sun,
487 J. (2017). Outcomes of Congenital Zika Disease Depend on Timing of Infection and Maternal-Fetal
488 Interferon Action. Cell Rep *21*, 1588-1599.

489 Corry, J., Arora, N., Good, C.A., Sadovsky, Y., and Coyne, C.B. (2017). Organotypic models of type
490 III interferon-mediated protection from Zika virus infections at the maternal-fetal interface. Proc Natl
491 Acad Sci U S A *114*, 9433-9438.

492 Denison, F.C., Kelly, R.W., Calder, A.A., and Riley, S.C. (1998). Cytokine secretion by human fetal
493 membranes, decidua and placenta at term. Hum Reprod *13*, 3560-3565.

494 Good, C., Wells, A.I., and Coyne, C.B. (2019). Type III interferon signaling restricts enterovirus 71
495 infection of goblet cells. Sci Adv *5*, eaau4255.

496 Guzeloglu-Kayisli, O., Guo, X., Tang, Z., Semerci, N., Ozmen, A., Larsen, K., Mutluay, D., Guller, S.,
497 Schatz, F., Kayisli, U.A.*, et al.* (2020). Zika Virus-Infected Decidual Cells Elicit a Gestational Age-

498 Dependent Innate Immune Response and Exaggerate Trophoblast Zika Permissiveness: Implication
499 for Vertical Transmission. J Immunol *205*, 3083-3094.

500 Haider, S., Meinhardt, G., Saleh, L., Kunihs, V., Gamperl, M., Kaindl, U., Ellinger, A., Burkard, T.R.,
501 Fiala, C., Pollheimer, J.*, et al.* (2018). Self-Renewing Trophoblast Organoids Recapitulate the
502 Developmental Program of the Early Human Placenta. Stem Cell Reports *11*, 537-551.

503 Jagger, B.W., Miner, J.J., Cao, B., Arora, N., Smith, A.M., Kovacs, A., Mysorekar, I.U., Coyne, C.B.,
504 and Diamond, M.S. (2017). Gestational Stage and IFN-lambda Signaling Regulate ZIKV Infection In
505 Utero. Cell Host Microbe *22*, 366-376 e363.

506 Laham, N., Brennecke, S.P., and Rice, G.E. (1997). Interleukin-8 release from human gestational
507 tissue explants: the effects of lipopolysaccharide and cytokines. Biol Reprod *57*, 616-620.

508 Lash, G.E., and Ernerudh, J. (2015). Decidual cytokines and pregnancy complications: focus on
509 spontaneous miscarriage. J Reprod Immunol *108*, 83-89.

510 Lazear, H.M., Schoggins, J.W., and Diamond, M.S. (2019). Shared and Distinct Functions of Type I
511 and Type III Interferons. Immunity *50*, 907-923.

512 Liu, J., Hao, S., Chen, X., Zhao, H., Du, L., Ren, H., Wang, C., and Mao, H. (2019). Human placental
513 trophoblast cells contribute to maternal-fetal tolerance through expressing IL-35 and mediating
514 iTR35 conversion. Nat Commun *10*, 4601.

515 McDonagh, S., Maidji, E., Chang, H.T., and Pereira, L. (2006). Patterns of human cytomegalovirus
516 infection in term placentas: a preliminary analysis. J Clin Virol *35*, 210-215.

517 Megli, C., Morosky, S., Rajasundaram, D., and Coyne, C.B. (2021). Inflammasome signaling in
518 human placental trophoblasts regulates immune defense against Listeria monocytogenes infection.
519 J Exp Med *218*.

520 Okae, H., Toh, H., Sato, T., Hiura, H., Takahashi, S., Shirane, K., Kabayama, Y., Suyama, M., Sasaki,
521 H., and Arima, T. (2018). Derivation of Human Trophoblast Stem Cells. Cell Stem Cell *22*, 50-63 e56.

522 Payne, A.F., Binduga-Gajewska, I., Kauffman, E.B., and Kramer, L.D. (2006). Quantitation of
523 flaviviruses by fluorescent focus assay. J Virol Methods *134*, 183-189.

524 Pereira, L., Maidji, E., McDonagh, S., Genbacev, O., and Fisher, S. (2003). Human cytomegalovirus
525 transmission from the uterus to the placenta correlates with the presence of pathogenic bacteria and
526 maternal immunity. J Virol *77*, 13301-13314.

527 Pitman, H., Innes, B.A., Robson, S.C., Bulmer, J.N., and Lash, G.E. (2013). Altered expression of
528 interleukin-6, interleukin-8 and their receptors in decidua of women with sporadic miscarriage. Hum
529 Reprod *28*, 2075-2086.

530 Platt, D.J., Smith, A.M., Arora, N., Diamond, M.S., Coyne, C.B., and Miner, J.J. (2018). Zika virus-
531 related neurotropic flaviviruses infect human placental explants and cause fetal demise in mice. Sci
532 Transl Med *10*.

533 Qiu, X., Zhu, L., and Pollard, J.W. (2009). Colony-stimulating factor-1-dependent macrophage
534 functions regulate the maternal decidua immune responses against Listeria monocytogenes
535 infections during early gestation in mice. Infect Immun *77*, 85-97.

536 Rizzuto, G., Tagliani, E., Manandhar, P., Erlebacher, A., and Bakardjiev, A.I. (2017). Limited
537 Colonization Undermined by Inadequate Early Immune Responses Defines the Dynamics of
538 Decidual Listeriosis. Infect Immun *85*.

539 Sheridan, M.A., Fernando, R.C., Gardner, L., Hollinshead, M.S., Burton, G.J., Moffett, A., and Turco,
540 M.Y. (2020). Establishment and differentiation of long-term trophoblast organoid cultures from the
541 human placenta. Nat Protoc *15*, 3441-3463.

542 Tabata, T., Petitt, M., Puerta-Guardo, H., Michlmayr, D., Wang, C., Fang-Hoover, J., Harris, E., and
543 Pereira, L. (2016). Zika Virus Targets Different Primary Human Placental Cells, Suggesting Two
544 Routes for Vertical Transmission. Cell Host Microbe *20*, 155-166.

545 Turco, M., Gardner, L., Koo, B., Moffett, A., & Burton, G. (2017). Derivation and long-term expansion
546 of human endometrial and decidual organoids. Protocol Exchange.

547 Turco, M.Y., Gardner, L., Hughes, J., Cindrova-Davies, T., Gomez, M.J., Farrell, L., Hollinshead, M.,
548 Marsh, S.G.E., Brosens, J.J., Critchley, H.O.*, et al.* (2017). Long-term, hormone-responsive organoid
549 cultures of human endometrium in a chemically defined medium. Nat Cell Biol *19*, 568-577.

550 Turco, M.Y., Gardner, L., Kay, R.G., Hamilton, R.S., Prater, M., Hollinshead, M.S., McWhinnie, A.,
551 Esposito, L., Fernando, R., Skelton, H.*, et al.* (2018). Trophoblast organoids as a model for maternal-
552 fetal interactions during human placentation. Nature *564*, 263-267.

553 Vassiliadis, S., Ranella, A., Papadimitriou, L., Makrygiannakis, A., and Athanassakis, I. (1998).
554 Serum levels of pro- and anti-inflammatory cytokines in non-pregnant women, during pregnancy,
555 labour and abortion. Mediators Inflamm *7*, 69-72.

556 von Rango, U., Classen-Linke, I., Raven, G., Bocken, F., and Beier, H.M. (2003). Cytokine
557 microenvironments in human first trimester decidua are dependent on trophoblast cells. Fertil Steril
558 *79*, 1176-1186.

559 Weisblum, Y., Oiknine-Djian, E., Vorontsov, O.M., Haimov-Kochman, R., Zakay-Rones, Z., Meir, K.,
560 Shveiky, D., Elgavish, S., Nevo, Y., Roseman, M.*, et al.* (2017). Zika Virus Infects Early- and
561 Midgestation Human Maternal Decidual Tissues, Inducing Distinct Innate Tissue Responses in the
562 Maternal-Fetal Interface. J Virol *91*.

563 Weisblum, Y., Panet, A., Zakay-Rones, Z., Haimov-Kochman, R., Goldman-Wohl, D., Ariel, I., Falk,
564 H., Natanson-Yaron, S., Goldberg, M.D., Gilad, R.*, et al.* (2011). Modeling of human cytomegalovirus
565 maternal-fetal transmission in a novel decidual organ culture. J Virol *85*, 13204-13213.

566 Wells, A.I., and Coyne, C.B. (2018). Type III Interferons in Antiviral Defenses at Barrier Surfaces.
567 Trends Immunol *39*, 848-858.

568 Yockey, L.J., Jurado, K.A., Arora, N., Millet, A., Rakib, T., Milano, K.M., Hastings, A.K., Fikrig, E.,
569 Kong, Y., Horvath, T.L.*, et al.* (2018). Type I interferons instigate fetal demise after Zika virus infection.
570 Sci Immunol *3*.

571 Zani, A., Zhang, L., McMichael, T.M., Kenney, A.D., Chemudupati, M., Kwiek, J.J., Liu, S.L., and
572 Yount, J.S. (2019). Interferon-induced transmembrane proteins inhibit cell fusion mediated by
573 trophoblast syncytins. J Biol Chem *294*, 19844-19851.
574

575

576

577

578

579

580

581

582

583

584

585

586

587

588

589

590

591

592 **Figure 1**
593

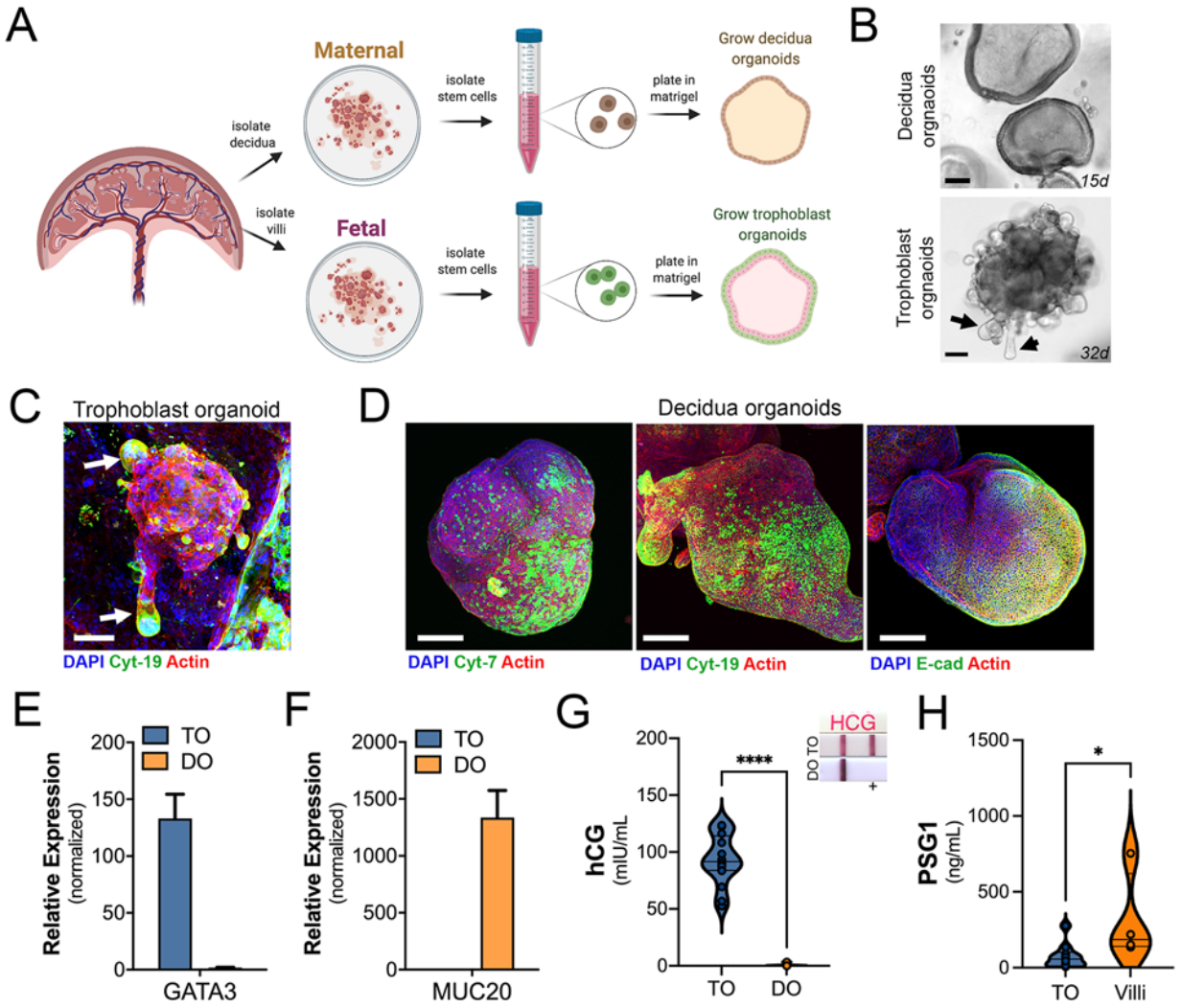

594
595
596

597 **Figure 1. Long-term three-dimensional organoids cultures can be established from human**
598 **mid- and late-gestation trophoblasts and decidua. (A)** Schematic representation of the derivation
599 of trophoblast organoids (TOs) and decidual organoids (DOs) from placental tissue. **(B)**
600 Representative bright-field images of TOs and DOs after passaging in complete growth medium
601 TOM and ExM, respectively at 15 days (DO, top) or 32 days (bottom) post-passaging . Scale bar, 50
602 µm. Black arrows denote placental-like villi extending from TOs (bottom). **(C)** Confocal microscopy
603 for cytokeratin-19 (Cyt-19, green), and actin (red) in a TO. DAPI-stained nuclei are in blue. Scale bar,
604 50 µm. White arrows denote placental-like villi. **(D)** Confocal microscopy for cytokeratin-7 (cyt-7,
605 green, left), cytokeratin-19 (Cyt-19, green, middle), or E-cadherin (E-cad, grren, right) and actin (red
606 in all) in DOs. DAPI-stained nuclei are in blue. Scale bar, 50 µm. **(E, F)** RT-qPCR analysis for the
607 trophoblast specific marker *GATA3* (E) or the decidual gland marker MUC20 (F) in matched TOs
608 (blue) and DOs (orange). Shown are the mean ± SD levels of expression normalized to *ACTB* and
609 normalized to DOs (E) or TOs (F). **(G)** Levels of hCG in conditioned medium (CM) isolated from TOs
610 (blue) or DOs (orange) as determined by ELISA. Each symbol represents an individual CM

preparation. Upper right shows the OTC pregnancy test stripe denoting an hCG positive line in TOs, but not DOs, after being placed into CM. **(H)** Levels of PSG-1 in conditioned medium (CM) isolated from TOs (blue) or chorionic villous explants (orange) as determined by ELISA. In (G) and (H) each symbol represents an individual CM preparation and significance was determined by Mann-Whitney U test. ****, $P < 0.0001$.

Figure 2

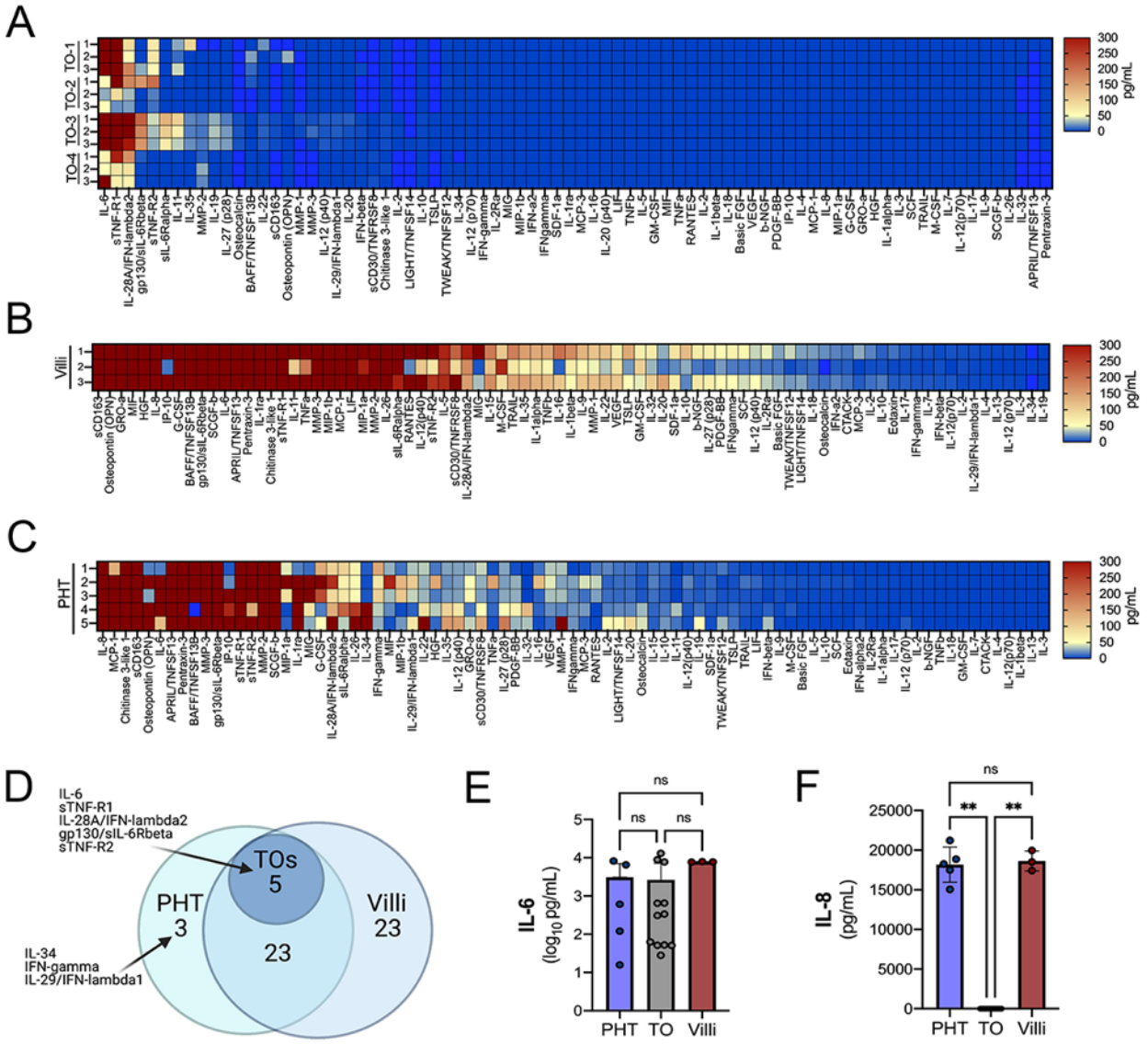

Figure 2. Cytokine secretion profiles from trophoblast organoids, matched placenta tissue, and primary cells. **(A)** Heatmap of twelve conditioned medium (CM) preparations generated from established TO lines analyzed by Luminex-based multianalyte profiling for the indicated cytokines, chemokines, and growth factors. Scale is shown at right. **(B)** Heatmap of CM generated from placental chorionic villi explants matched to TOs shown in A. Luminex assays were performed from three independent CM preparations. Scale is shown at right. **(C)** Heatmap of CM generated from primary human trophoblast cells cultured from full-term placentas. Luminex assays were performed from five independent CM preparations. Scale is at right. **(D)** Venn diagram showing the overlap of detectable factors in TOs, matched placenta chorionic villi, and primary cells from A-C. **(E, F)** Concentrations and comparison of the levels of IL-6 (E) and IL-8 (F) in CM from TOs (grey), matched chorionic villi (dark red), and primary cells (blue) shown in A-C. Each symbol represents a unique

CM preparation. Significance was determined by Kruskal Wallace U test with multiple comparisons. **, $P < 0.01$; ns, not significant.

Figure 3

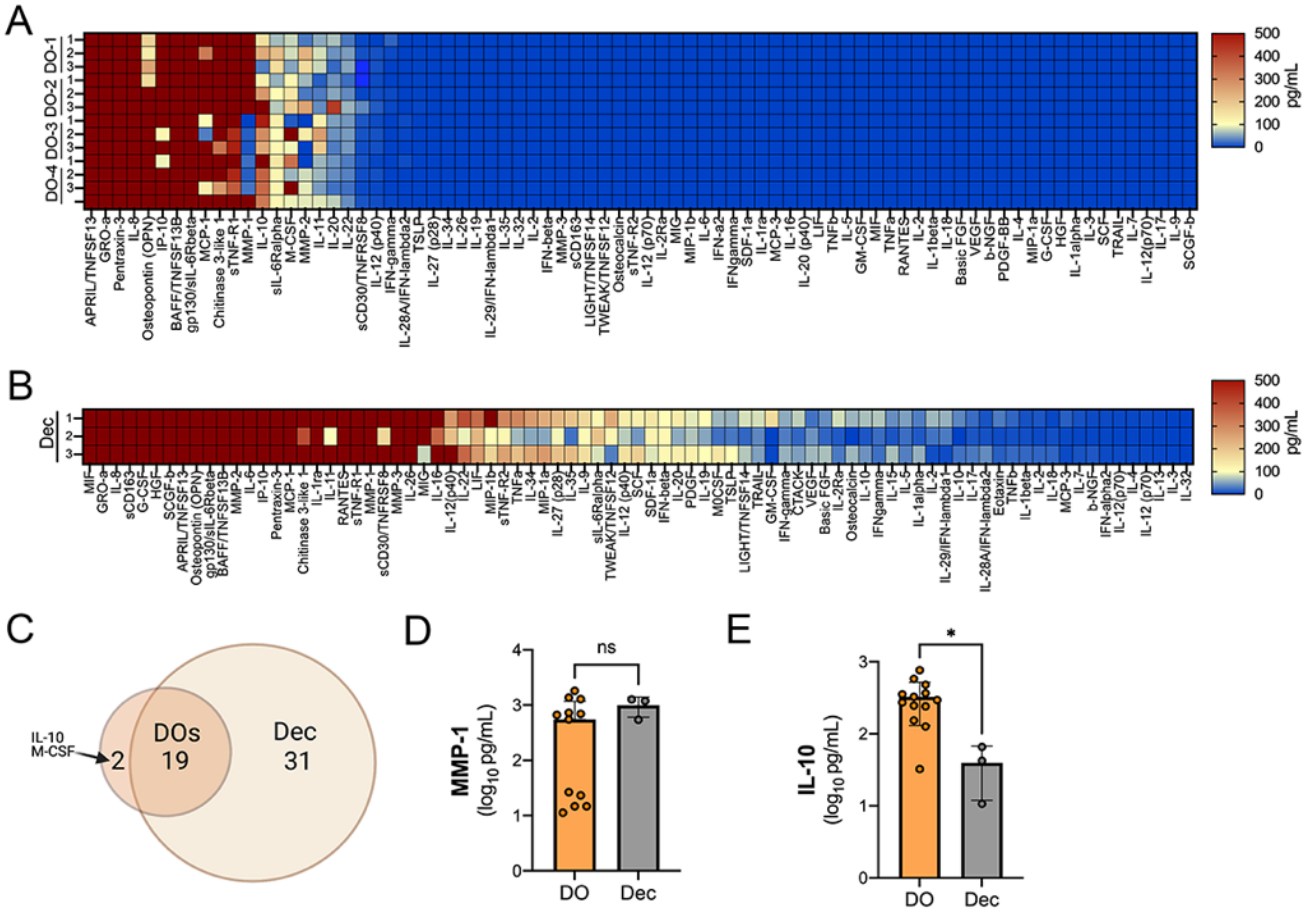

Figure 3. Cytokine secretion profiles from decidua organoids and decidua tissue. **(A)** Heatmap of twelve CM preparations generated from established DO lines analyzed by Luminex-based multianalyte profiling. Scale is at right. **(B)** Heatmap of CM generated from three independent decidual explants (two of these, at top and middle, are matched to DOs shown in A). Luminex assays were performed from three independent CM preparations. Scale is shown at right. **(C)** Venn diagram showing the overlap of detectable factors in CM isolated from DOs and decidual tissues. **(D, E)** Concentrations and comparison of the levels of MMP-1 (D) and IL-10 (E) in CM from DOs (orange) and decidual tissues (grey) shown in A and B. Each symbol represents a unique CM preparation. Significance was determined by Mann-Whitney U test. *, $P < 0.05$; ns, not significant.

Figure 4

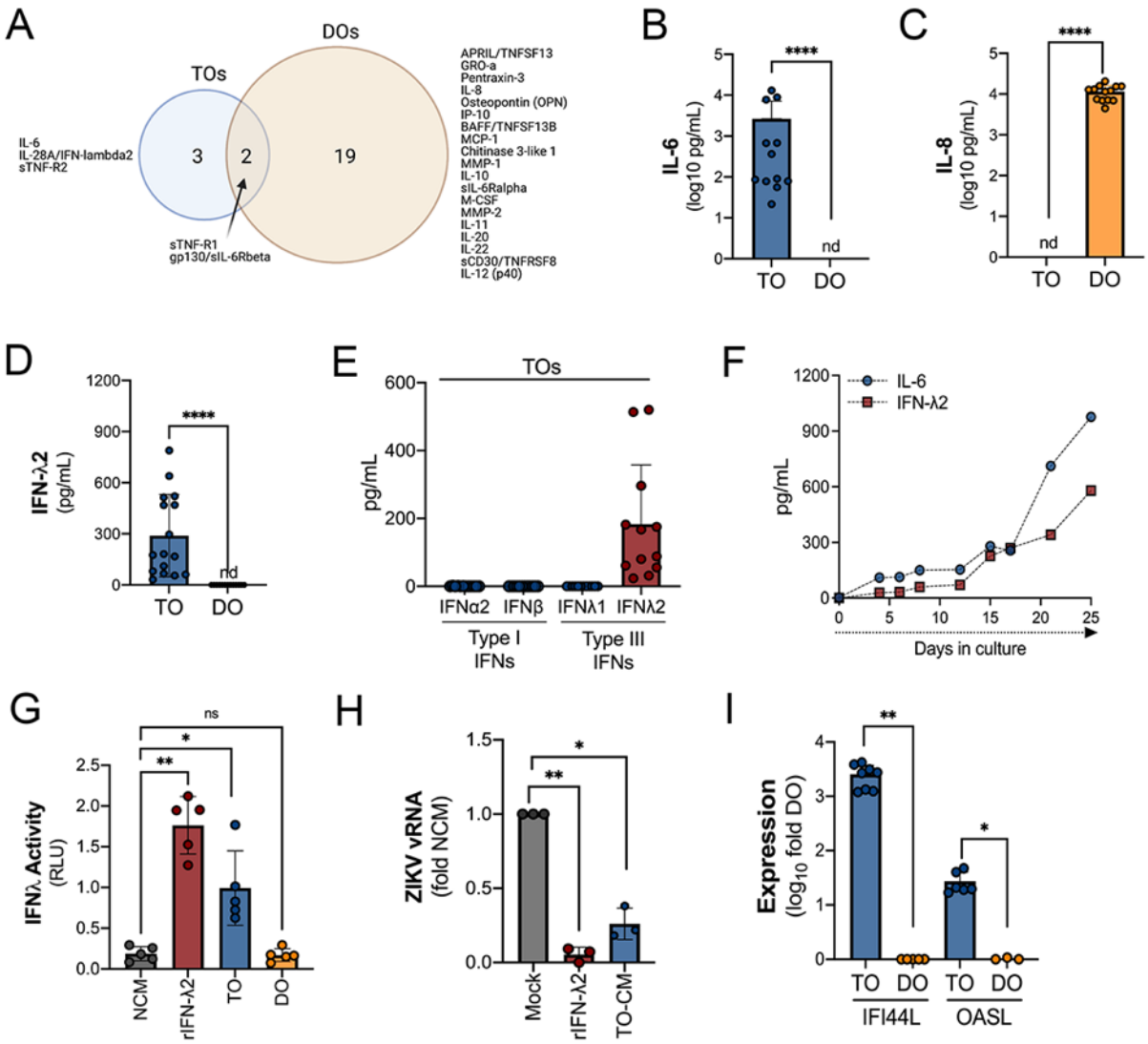

Figure 4. Trophoblast organoids preferentially secrete high levels of antiviral IFN-λ2. **(A)** Venn diagram comparing the factors identified in CM isolated from TOs and DOs. **(B, C)** Concentrations and comparison of the levels of IL-6 (B) and IL-8 (C) released by TOs (blue) and DOs (orange) determined by Luminex-based profiling. Each symbol represents a unique CM preparation. **(D)** Comparison of the levels of IFN-λ2 in CM isolated from TOs (blue) and DOs (orange) as determined by Luminex. **(E)** Comparison of the levels of the type I IFNs IFN-α2 and IFN-β and type III IFNs IFN-λ1 and IFN-λ2 in CM isolated from TOs. **(F),** Concentrations of IL-6 (blue) and IFN-λ2 (red) in CM generated from a single TO line throughout the first 25 days of culture. **(G)** IFN-λ activity of CM isolated from TOs (blue) and DOs (orange) as assessed using an IFN-λ reporter 293T cells line. NCM (non-conditioned medium, grey) was as negative control, NCM supplemented with recombinant human IFN-λ2 (100ng) was used as a positive control (red). **(H)** Human osteosarcoma

U2OS cells were treated with CM isolated from TOs (blue) or with recombinant IFN-λ2 (100ng) for 24hrs and then infected with ZIKV for 24hrs (in the presence of CM). Level of ZIKV replication was assessed by viral RNA as determined by qPCR. Data are shown as fold change from NCM and from at least three independent CM preparations. **(I)** RT-qPCR analyses for two ISGs, IFI44L and OASL in TOs (blue) and DOs (orange). Data are shown as fold change from DOs and from at least three independent replicates. In B–H, each symbol represents unique CM preparations. In I, each symbol represents individual replicates (technical and experimental). Significance was determined by Mann-Whitney U test or by Kruskal Wallace U test with multiple comparisons. *, $P < 0.05$; **, $P < 0.01$; ****, $P < 0.0001$.

Figure 5

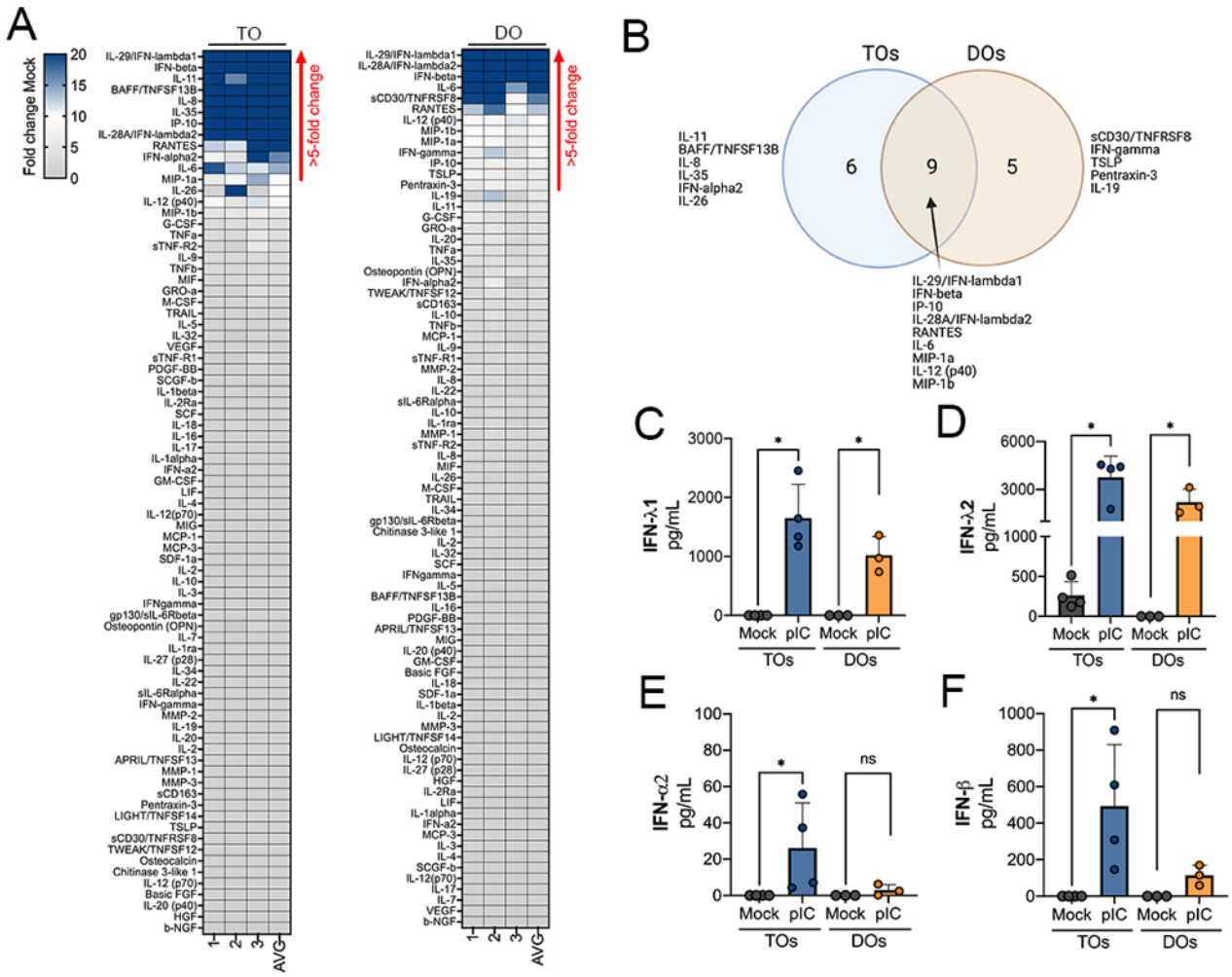

Figure 5. Differential cytokine release in TOs and DOs treated with poly I:C. (A) Heatmaps demonstrating the induction of factors at left (shown as fold change from mock-treated controls) from TOs (left panel) and DOs (right panel) treated with 10μg poly (I:C) and analyzed by multiplex Luminex-based profiling. AVG denotes the average change in concentration of factors over CMs from individual preparations. Dark blue denotes significantly induced factors compared with untreated controls. Gray or white denotes little to no change (scale at top left). The red arrow demonstrates factors with induction greater than five-fold change observed in the average of separate experiments. Data are from four individual CM preparations from at least two unique matched organoid lines. **(B)** Venn diagram showing overlap of the factors released >5-fold by poly I:C treatment in TOs and DOs. **(C-F)** Levels of IFN-λ1 (C), IFN-λ2 (D) IFN-α2 (E), and IFN-β (F) in CM isolated from poly I:C-treated TOs (blue) and DOs (orange) or in mock-treated controls (grey). In C-F, each symbol represents individual CM preparations. In C-F significance was determined using a Mann-Whitney U test. *, $P < 0.05$; ns, not significant.

Figure 6

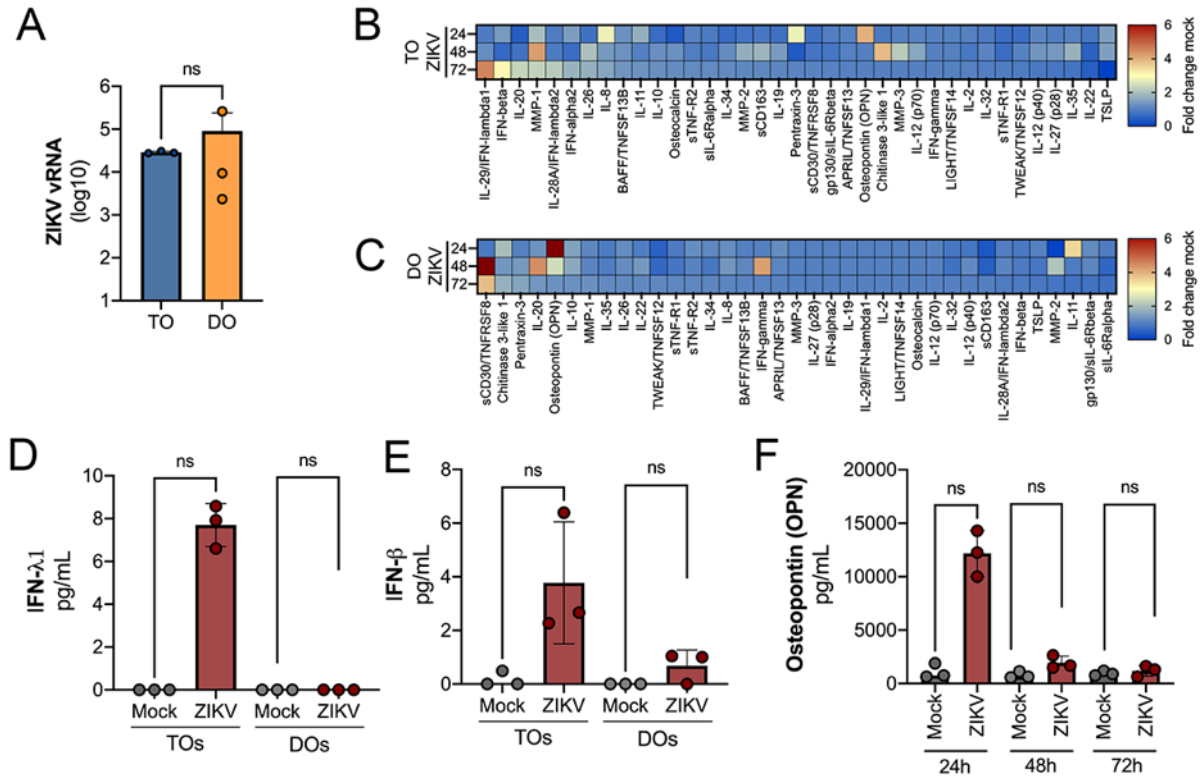

Figure 6. **Differential cytokine release in TOs and DOs infected with ZIKV**. **(A)** ZIKV replication in TOs (blue) and DOs (red) was assessed by the production of vRNA by RT-qPCR 72hrs post-infection. Data are shown as fold change from mock controls. **(B, C)** Heatmaps demonstrating the induction of cytokines in CM (shown as fold change from mock controls) collected from TOs (B) and DOs (C) infected with ZIKV for indicated hours (24 to 72 hours) analyzed by multiplex Luminex-based profiling. Scale is shown at right. **(D, E**) Concentrations of IFN-λ1 (D) and IFN-β (E) in CM generated from TOs and DOs infected with ZIKV for 72 hrs (dark red) or in mock-treated controls (grey). **(F)** Concentrations osteopontin in CM generated from DOs infected with ZIKV for the indicated time (dark red) or in mock infected controls (mock, grey). In D-F, each symbol represents individual CM preparation. Significance was determined with Mann-Whitney U test. ns, not significant.

845
846 **Figure 7**
847

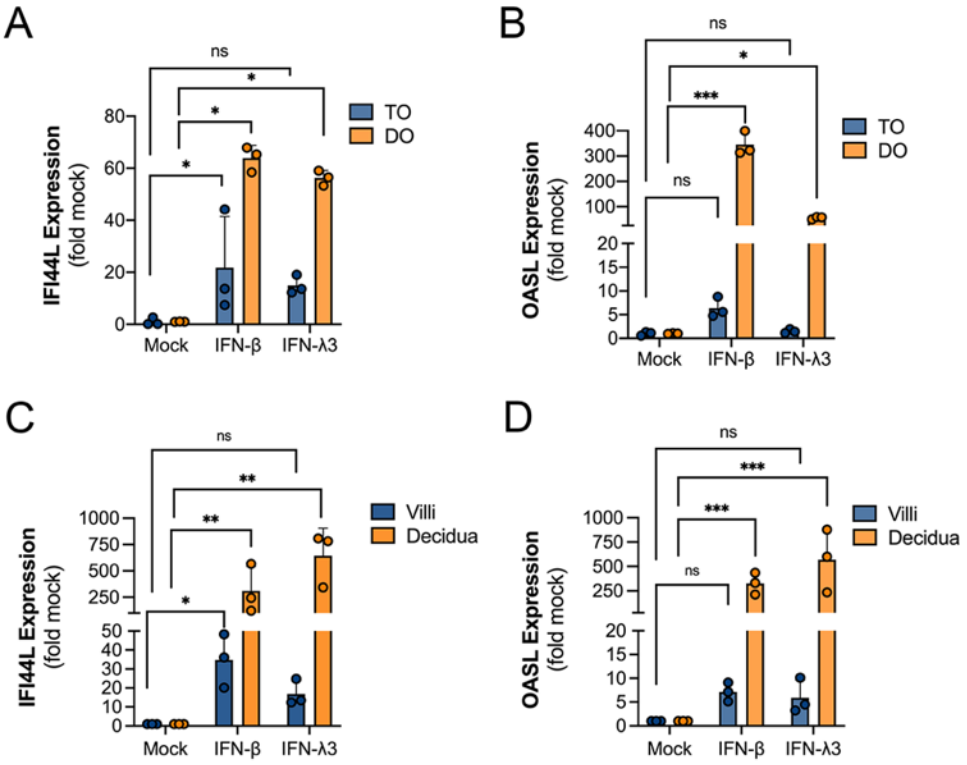

848
849
850 **Figure 7**. **Responses of TOs and DOs and placental tissue to recombinant IFNs. (A, B)** RT-
851 qPCR analyses for two ISGs, IFI44L (A) and OASL(B) in TOs (blue) and DOs (orange) treated with
852 100ng recombinant human IFN-β or IFN-λ3 treatment for ~24 hours. Data are shown as fold change
853 from mock-treated controls two independent replicates performed in triplicate. **(C, D),** RT-qPCR
854 analyses for IFI44L (C) and OASL(D) in chorionic villous (blue) or decidua (orange) explants treated
855 100ng recombinant human IFN-β or IFN-λ3 treatment for ~24 hours. Significance was determined
856 by Kruskal Wallace U test with multiple comparisons. *, $P < 0.05$; ***;**, $P < 0.01$; $P < 0.001$; ns, not
857 significant.
858
859
860
861
862
863
864
865
866
867
868
869

870
871 **Table S1. qPCR primers used in this study.**

Target	Forward, 5'→3'	Reverse, 5'→3'
Actin	ACTGGGACGACATGGAGAAAAA	GCCACACGCAGCTC
IFN-β	GAGCTACAACTTGCTTGGATTC	CAAGCCTCCCATTCAATTGC
IFN-λ2	ACATAGCCCAGTTCAAGTC	GACTCTTCTAAGGCATCTTTG
IFI44L	AACCTAGACGACATAAAGAGG	CTGAAACCAAGTCTGCATAG
OASL	GTACCAGCAGTATGTGAAAG	ATGGTTAGAAGTTCAAGAGC
GATA3	AAAATGAACGGACAGAACC	GGGGTCTGTTAATATTGTGAAG
MUC20	CTCTTCCTTCTGTCCCTC	CCATTTTCACCTGCACTC
ZIKV	AGATGACTGCGTTGTGAAGC	GAGCAGAACGGGACTTCTTC

872
873
874
875
876
877
878
879
880
881
882
883
884
885
886
887
888
889
890
891
892
893
894
895
896
897
898
899
900
901
902

Supplemental Figure 1

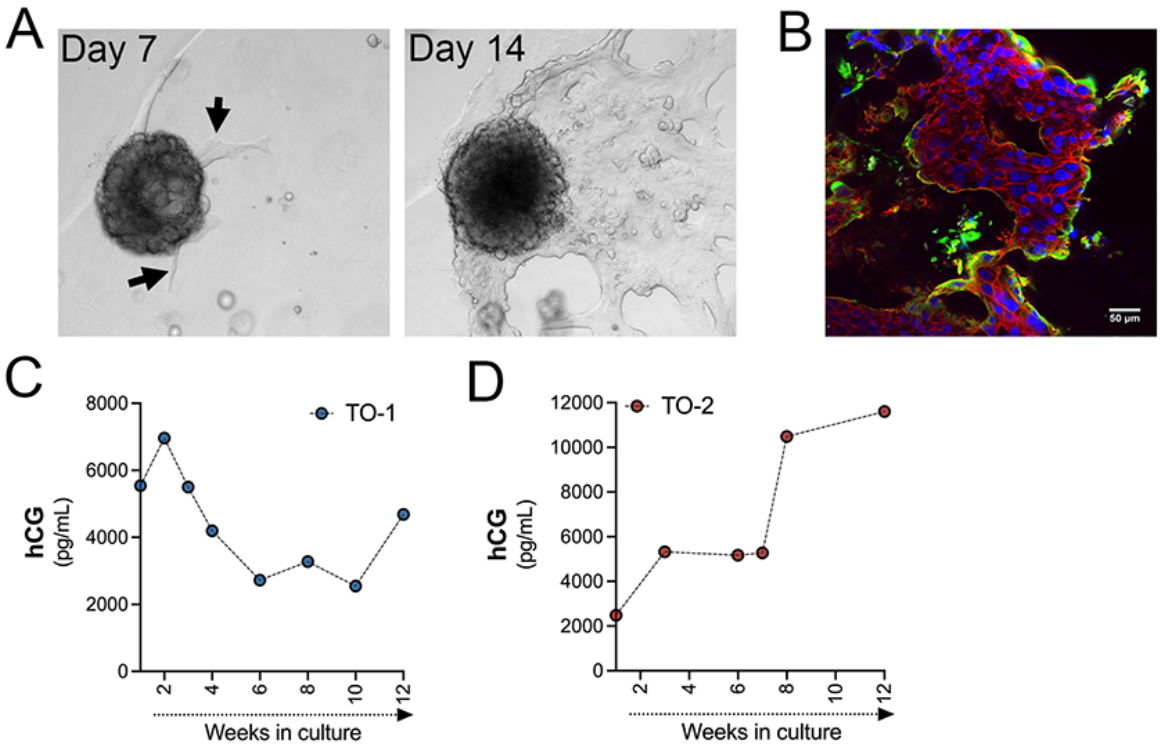

Supplemental Figure 1. **(A),** Brightfield image of a TO at 7 or 14 days post-plating. Black arrows denote EVTs that migrate from the organois to invade surrounding Matrigel. **(B),** Confocal micrograph of EVTs growing from a TO and immunostained for cytokeratin-19 (green) and actin (red). DAPI-stained nuclei are shown in blue. **(C, D)** hCG levels as assessed by ELISA in conditioned medium isolated from two TOs lines isolated at the indicated weeks during culture.
.

927
928
929 **Supplemental Figure 2**
930
931

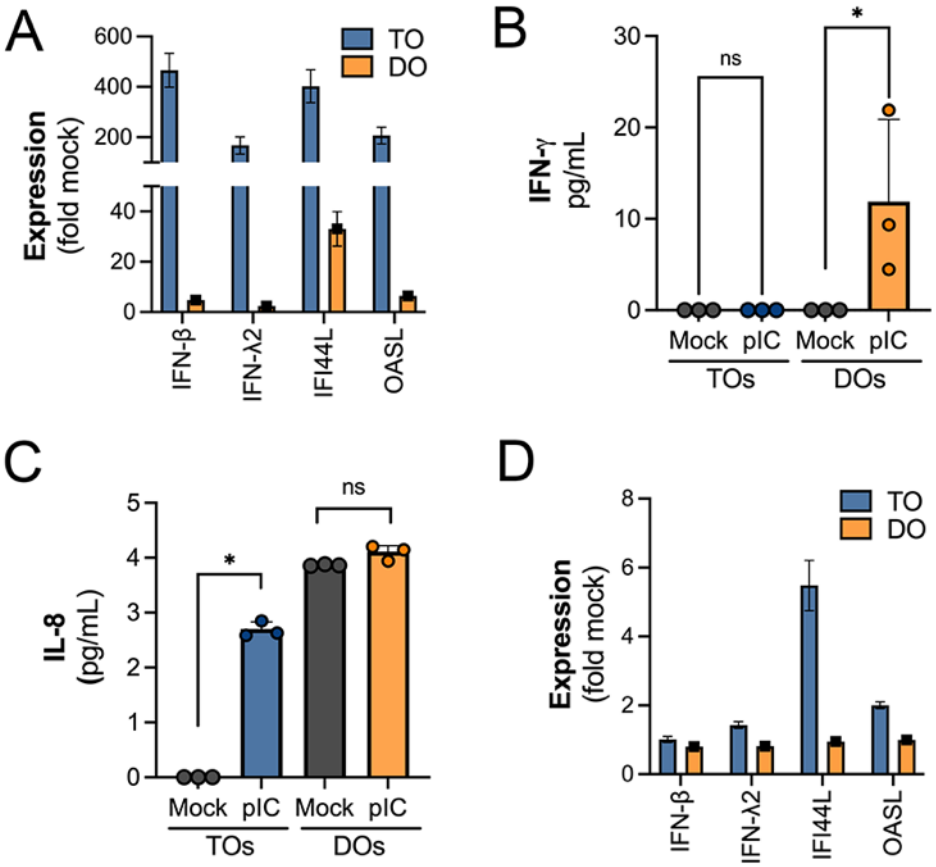

932
933 **Supplemental Figure 2. (A),** RT-qPCR for IFN-β, IFNλ-2, IFI44L, and OASL in poly I:C treated TOs
934 (blue) and DOs (orange). Data are shown as mean ± standard deviation as a fold change from mock-
935 treated controls. **(B, C),** Levels of IFN-γ (B) or IL-8 (C) as assessed by Luminex in TOs (blue) and
936 DOs (orange) treated with poly I:C or in mock-treated controls (grey). Data are shown as mean ±
937 standard deviation. Symbols represents unique organoid preparations. **(D),** RT-qPCR for IFN-β,
938 IFNλ-2, IFI44L, and OASL in ZIKV-infected TOs (blue) and DOs (orange) 72hrs post-infection. Data
939 are shown as mean ± standard deviation as a fold change from mock-infected controls. Significance
940 was determined with Mann-Whitney U test. *, $p<0.05$, ns, not significant.
941
942
943
944
945
946